Angular dependence of the response of the nanoDot OSLD system for measurements at depth in clinical megavoltage beams

Joerg Lehmann[a)]
Australian Clinical Dosimetry Service, 619 Lower Plenty Road, Yallambie, VIC 3085, Australia; Institute of Medical Physics, University of Sydney, Physics Road A28, Sydney, NSW 2006, Australia; and School of Applied Sciences, Royal Melbourne Institute of Technology (RMIT) University, GPO Box 2476, Melbourne, VIC 3000, Australia

Leon Dunn, Jessica E. Lye, John W. Kenny, Andrew D. C. Alves, and Andrew Cole
Australian Clinical Dosimetry Service, 619 Lower Plenty Road, Yallambie, VIC 3085, Australia

Andre Asena
School of Chemistry, Physics and Mechanical Engineering, Queensland University of Technology, Brisbane, QLD 4001, Australia

Tomas Kron
Australian Clinical Dosimetry Service, 619 Lower Plenty Road, Yallambie, VIC 3085, Australia; School of Applied Sciences, Royal Melbourne Institute of Technology (RMIT) University, GPO Box 2476, Melbourne, VIC 3000, Australia; and Peter MacCallum Cancer Centre, St Andrews Place, East Melbourne, VIC 3002, Australia

Ivan M. Williams
Australian Clinical Dosimetry Service, 619 Lower Plenty Road, Yallambie, VIC 3085, Australia and School of Applied Sciences, Royal Melbourne Institute of Technology (RMIT) University, GPO Box 2476, Melbourne, VIC 3000, Australia

(Received 15 January 2014; revised 23 April 2014; accepted for publication 27 April 2014; published 20 May 2014)

Purpose: The purpose of this investigation was to assess the angular dependence of a commercial optically stimulated luminescence dosimeter (OSLD) dosimetry system in MV x-ray beams at depths beyond d_{max} and to find ways to mitigate this dependence for measurements in phantoms.
Methods: Two special holders were designed which allow a dosimeter to be rotated around the center of its sensitive volume. The dosimeter's sensitive volume is a disk, 5 mm in diameter and 0.2 mm thick. The first holder rotates the disk in the traditional way. It positions the disk perpendicular to the beam (gantry pointing to the floor) in the initial position (0°). When the holder is rotated the angle of the disk towards the beam increases until the disk is parallel with the beam ("edge on," 90°). This is referred to as Setup 1. The second holder offers a new, alternative measurement position. It positions the disk parallel to the beam for all angles while rotating around its center (Setup 2). Measurements with five to ten dosimeters per point were carried out for 6 MV at 3 and 10 cm depth. Monte Carlo simulations using GEANT4 were performed to simulate the response of the active detector material for several angles. Detector and housing were simulated in detail based on microCT data and communications with the manufacturer. Various material compositions and an all-water geometry were considered.
Results: For the traditional Setup 1 the response of the OSLD dropped on average by 1.4% ± 0.7% (measurement) and 2.1% ± 0.3% (Monte Carlo simulation) for the 90° orientation compared to 0°. Monte Carlo simulations also showed a strong dependence of the effect on the composition of the sensitive layer. Assuming the layer to completely consist of the active material (Al_2O_3) results in a 7% drop in response for 90° compared to 0°. Assuming the layer to be completely water, results in a flat response within the simulation uncertainty of about 1%. For the new Setup 2, measurements and Monte Carlo simulations found the angular dependence of the dosimeter to be below 1% and within the measurement uncertainty.
Conclusions: The dosimeter system exhibits a small angular dependence of approximately 2% which needs to be considered for measurements involving other than normal incident beams angles. This applies in particular to clinical *in vivo* measurements where the orientation of the dosimeter is dictated by clinical circumstances and cannot be optimized as otherwise suggested here. When measuring in a phantom, the proposed new setup should be considered. It changes the orientation of the dosimeter so that a coplanar beam arrangement always hits the disk shaped detector material from the thin side and thereby reduces the angular dependence of the response to within the measurement uncertainty of about 1%. This improvement makes the dosimeter more attractive for clinical measurements with multiple coplanar beams in phantoms, as the overall measurement uncertainty is reduced. Similarly,

phantom based postal audits can transition from the traditional TLD to the more accurate and convenient OSLD. [http://dx.doi.org/10.1118/1.4875698]

Key words: optically stimulated luminescence dosimeter (OSLD), angular dependence of response, radiation measurement, radiotherapy audits, quality assurance (QA) measurements

1. INTRODUCTION

This work addresses the angular dependence of the response of the nanoDot™ dosimetry system (Landauer Inc., Glenwood, IL) for the application in phantoms at a depth beyond d_{max} with MV x rays. The system uses optically stimulated luminescence dosimeter (OSLD) in a small plastic casing (nanoDOT). Principles and details of OSLD have been reported in Refs. 1–5.

OSLDs have a variety of applications in Medical Physics.[6–14] They are used in phantom measurements performed when implementing new techniques into clinical practice and for individual patient quality assurance (QA) procedures. Often, the dosimeters are located inside a phantom and can receive radiation from multiple fields and directions, making angular dependence of their response important.

For many clinical audits, passive detectors such as OSLD nanoDots, are also placed inside plastic phantoms. For higher level audits, in particular for Level III end-to-end tests, the dosimeters are located in the body of an anthropomorphic phantom to be irradiated from multiple directions,[15] again making angular dependence of their response important. In Level I audits[16] (machine output check) the beam is directed normal to the OSLD, making their angular response less significant here.

Angular dependence for measurements at depth is also important for clinical *in vivo* measurements. For *in vivo* clinical measurements in external beam radiation therapy, the dosimeters are generally placed on the patient's skin. Often bolus material is attached over the dosimeter to establish a more favorable electron equilibrium condition at the location of the detector material. Clinical measurements are performed for single electron fields and for single and multibeam photon treatments. In the case of single field measurements, the direction of the beam is often not normal to the surface of the detector. It is therefore of interest to what magnitude this deviation from a normal angle impacts the response of the detector, which is calibrated with a normal beam. In multibeam arrangements, similar non-normal irradiation is inevitable, raising the same angular dependency issues.

The dosimeter manufacturer states that the dosimeters feature "minimal angular dependence."[17] Jursinic reported from his detailed experiments that the dosimeters show "no angular dependence within the measurement uncertainty."[1] In a paper that covered many properties of OSLD, Jursinic investigated responses for 24 incident angles (15° steps). Using a 6 MV beam (field size 10 × 10 cm^2), he performed comprehensive measurements in water equivalent custom phantoms with the dosimeter positioned at approximately 1.8 cm depth. The data in Fig. 7 of his paper[1] show angular responses for OSLD which differ up to 2% from unity in both directions, relative to the response for the beam angle normal to the front surface of the dosimeter. Jursinic reported a measurement uncertainty of 0.9% (one standard deviation).

Recently, Kerns *et al.*[18] demonstrated through experiment and Monte Carlo simulation that nanoDots do exhibit an angular dependence. Their study showed a 4% drop in signal for 6 MV photon beams at approximately 10 cm depth (3% for 18 MV) for nanoDot orientations of 90° (edge on to beam) compared with nanoDot irradiated straight on.

Kim *et al.*[19] investigated angular dependence of the response of the nanoDot OSLD for angles up to 75° with measurements at depth and at the surface of a phantom. For the setup at depth, where the detector was at the center of a 30 cm diameter cylindrical phantom, the group found a drop in signal of 2.4% for 75° vs 0° for 6 MV photon beams. In their second setup, Kim *et al.* placed the dosimeters on the surface of a stack of solid water, simulating a dosimeter on the patient's skin (without any bolus). Here, the results for the 6 MV photon beam showed an increase in dosimeter response of 70% for 75° vs 0°. For 6 MeV electrons the increase was 9% for 50° and 5.1% for 75° compared to the 0° angle.

Based on the above cited studies and the nonspecific statement of the manufacturer, the angular response of the nanoDOT OSL dosimeter is not well known. While there is data indicating an increased response of up to 4% for the edge on orientation (90°) compared to the straight on orientation (0°) other work states that there is no dependence. As a variation in the response of a dosimeter in a magnitude of up to 4% can make an important difference in dosimetry for clinical QA, *in vivo* dosimetry, and audit measurements this study was designed. Its purpose was to carefully examine the angular dependence of the response of the nanoDot OSL dosimeter in photon beams at depth and to develop methods to mitigate any dependence. The study employed measurements in MV photon beams with newly designed custom phantom inserts and comprehensive Monte Carlo simulations.

2. MATERIAL AND METHODS

2.A. Experimental methods

2.A.1. Design of dosimeter holder

The measurements in this study were performed using an anthropomorphic phantom with removable, cylindrical rods (IMRT Phantom Model 002LFC CIRS, Norfolk, VA). Two special holders (rods) were designed and built from Plastic Water™ (CIRS Inc., Norfolk, VA), the same material as the rod in the phantom they were replacing for the measurements.

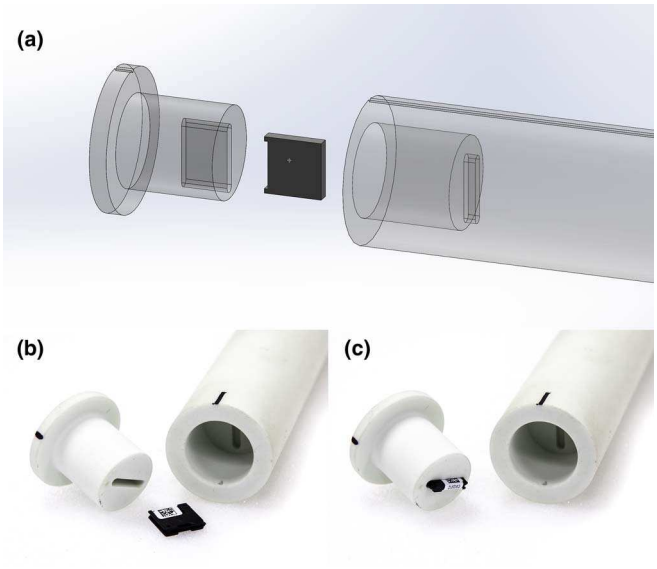

FIG. 1. Custom CIRS Plastic Water^{TM} rod machined to hold a nanoDOT OSLD with the center of the detector material at the rod's center of rotation in longitudinal direction for "Setup 1." In this, the traditional setup, the beam direction is normal to the largest detector surface (bar code side facing the beam) at angle = 0°. Marks on the outside of the rod correspond with the orientation of the detector. (a) A drawing of the custom rod that was used in the computer aided design process, illustrating cavities and dosimeter position; (b) and (c) photographs of the finished device without and with a dosimeter in place, respectively. See Fig. 2 for a schematic illustration of beam direction and dosimeter rotation.

The holders have been machined to hold one nanoDot OSLD in a way that it can be rotated while the center of the OSLD detector material is at the center of rotation of the rod in longitudinal direction.

The first holder rotates the disk in the traditional way. It positions the disk perpendicular to the beam (gantry pointing to the floor) in the initial position (0° per chosen nomenclature). In other words, the detector faces the beam at angle = 0° orientation when the beam direction is normal to the largest detector surface with the bar code side of the dosimeter facing the beam. When the holder is rotated the angle of the detector disk towards the beam increases until the disk is parallel with the beam ("edge on," 90°). Marks on the outside of the rod correspond with the orientation of the detector direction (Fig. 1). For each measurement the rod was aligned to the corresponding angle using an angular scale marked on the phantom body. This arrangement is henceforth referred to as "Setup 1." Figure 2(a) illustrates the position of the detector with respect to the beam and the axis of rotation.

With the goal to mitigate angular dependence, the study also investigated the angular dependence of the response of the dosimeter when the detector is positioned parallel to the axial patient plane and thereby for each beam angle oriented with an edge towards the beam. While a reduced response was expected compared to an *enface* irradiated dosimeter, the aim was to see whether the response was consistent through all angles. This new dosimeter orientation could be implemented for commissioning, clinical patient specific QA, and in audit situations, when the dosimeter is placed inside a plastic phantom. It would not be feasible for most clinical *in vivo* measurements.

A second dosimeter holder was machined to place the nanoDOT in axial direction (Fig. 3). When the holder is placed in the phantom, the beam strikes the dosimeter on its side for each angle. Again, the center of the detector material is at the center of rotation in longitudinal direction. This, new positioning of the detector is referred to as "Setup 2."

2.A.2. Measurements on linear accelerator

Measurements were performed with an Elekta Synergy linear accelerator (Elekta AB, Stockholm, Sweden). Dosimeters were exposed in the phantom (Fig. 4) in a 100 cm SSD setup with 100 MU per exposure using a 10 × 10 cm^2 field at

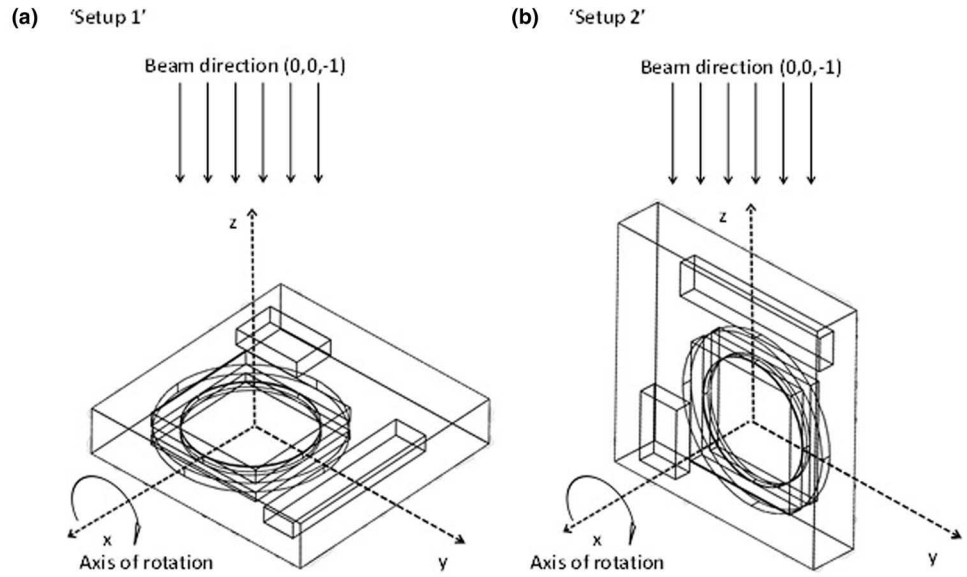

FIG. 2. Schematic of position and angles of rotation of the detector with respect to the beam for (a) Setup 1 and (b) Setup 2.

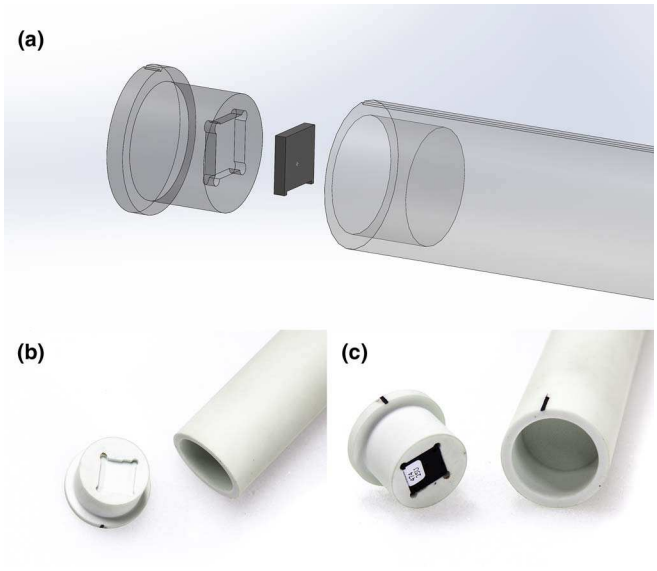

FIG. 3. Custom CIRS Plastic Water^{TM} rod machined to hold a nanoDOT OSLD in axial direction. The center of the detector material is located at the rod's center of rotation in longitudinal direction for "Setup 2." In this new approach the beam is always perpendicular to the largest detector surface. Marks on the outside of the rod corresponded with the orientation of the detector. See Fig. 2 for a schematic illustration of beam direction and dosimeter rotation. (a) A drawing of the custom rod that was used in the computer aided design process illustrating cavities and dosimeter position; (b) and (c) photographs of the finished device without and with a dosimeter in place, respectively.

gantry and collimator angles set to 0°. The phantom was positioned laterally in the A-B axis with inserts open to the A side. Using marks on the outside of the custom rod, each dosimeter was brought into the desired angular position with respect to the beam. For Setup 1, measurements were performed at two depths: 3 and 10 cm (center of OSLD detector material). The depth of 3 cm was chosen as a shallow depth, where

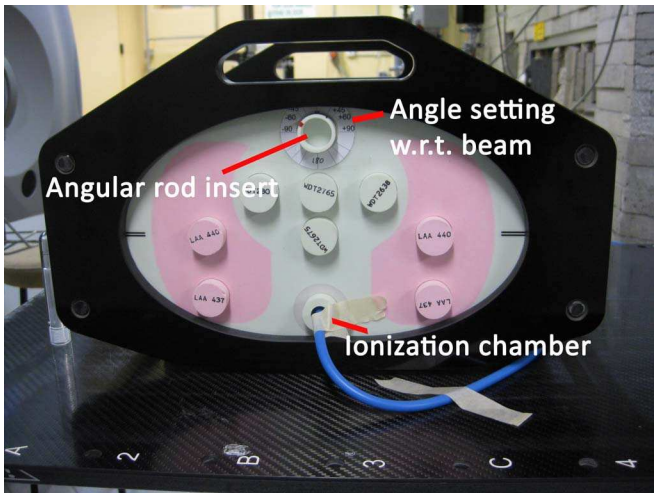

FIG. 4. CIRS Phantom Model 002LFC with custom rod (top) at the 3 cm depth position. Using marks on the outside of the rod, the dosimeter was brought into the desired angular position with respect to the beam. A Farmer chamber with a suitable insert (bottom, middle) was used to monitor machine output. Other measurements were performed with the OSLD at 10 cm depth, two positions down from the shown position.

conceptually the photons of the incoming beam are less scattered and any angular dependence of the detector response should be expressed more strongly. The depth of 10 cm was chosen for comparison with some of the published data. For both depths, measurements were performed for three orientations (−90°, 180°, 90°) following the nomenclature described above. Ten dosimeters were exposed at every measurement point.

All dosimeter readings were corrected with previously determined element correction factors, describing the response of a dosimeter relative to the batch average.[5] The average readings of the dosimeters for each angle were used to find the mean and standard deviation of the relative response for that angle. Ion chamber measurements with a Farmer chamber were used to monitor the linac output.

For Setup 2, measurements were performed at a depth of 3 cm (center of OSLD detector material). For this setup five orientations were investigated (−90°, −45°, 0°, 45°, 90°), covering the potential impact of the nonsymmetric internal structure of the dosimeter. Five dosimeters were used per orientation. The same readout and analysis procedures were performed as for Setup 1.

2.B. Geant4 Monte Carlo simulations

Monte Carlo simulations using Geant4 (Ref. 20) were performed to simulate the response of the active detector material. The Geant4 simulation geometry consisted of a simulated nanoDot dosimeter in a 30 × 30 × 30 cm^3 block of water. Simulations were performed for both orientations of the dosimeter (perpendicular—Setup 1 and parallel—Setup 2) at depths 3 and 10 cm. The rotation of the dosimeter was about the center of the detector material simulating the experimental setups.

The geometry and materials of the dosimeter, its housing and air gaps were considered in detail, based on earlier experience of Charles *et al.*,[21] correspondence with the manufacturer and studies of micro-CT images of the dosimeter. Ten nanoDOT dosimeters were imaged with a micro-CT (SCANCO Medical AG, Basserdorf, Switzerland, nominal x-ray energy: 55 kVp, tube current: 145 μA, 20 μm isotropic resolution). The dimensions and densities of the imaged dosimeters were analyzed and formed the basis for the dosimeter details used in the simulations, as described below. Figure 5 shows selected views of a dosimeter from the micro-CT scans.

Figure 6 shows the simulation geometry. The outer casing of the dosimeter was modeled as a rectilinear polygon of water equivalent material with a density override to 1.03 g/cm^3 and dimensions of 10 × 10 × 2 mm^3. Inside the outer case four air gaps are modeled mimicking the actual air gaps as seen in the micro-CT. The sensitive volume of the dosimeter is a disk of 5 mm diameter and a thickness of 0.2 mm. It is positioned offset by 1 mm relative to the center of the housing in both of the long dimensions. The detector disk consists of a mixture of aluminium oxide (Al_2O_3:C) and a polyester-binder sandwiched in-between a polyester substrate (0.2 mm thick) and polyester film coating (0.05 mm thick). The composition

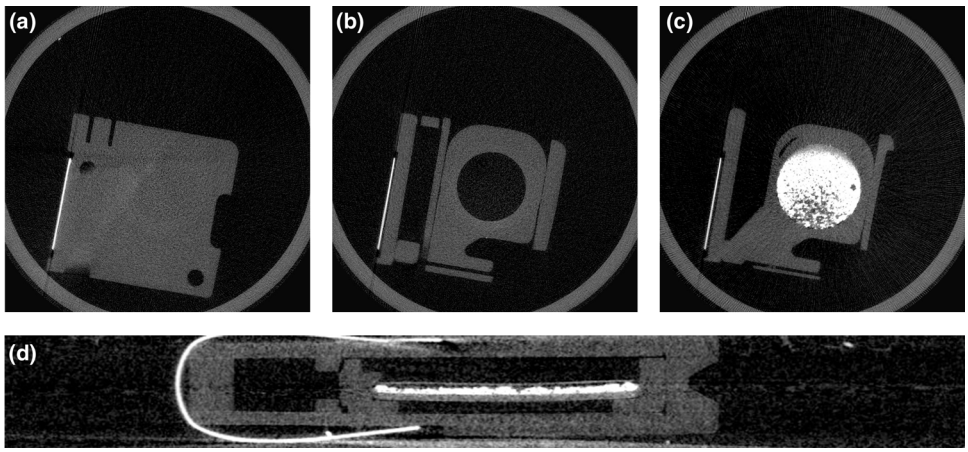

FIG. 5. Micro-CT images of the internal structure of a nanoDOT OSLD used as basis for the details of the simulation geometry (SCANCO Medical AG, Basserdorf, Switzerland, nominal x-ray energy: 55 kVp, tube current: 145 μA, 20 μm isotropic resolution). (a), (b), and (c) Axial slices showing the housing, an internal part without detector material, and a central part with detector material (brighter due to its higher density), respectively. (d) A coronal slice at larger scale.

of the detector disk has been modeled as 78.4% Al_2O_3 (ρ = 3.96 g/cm^3) and 21.6% polyester (ρ = 1.18 g/cm^3). The sensitive material also contains a very small amount (0.01%–0.5%) of carbon doping,[22] which has not been considered in the simulations. The effective density of the detector disk is 1.41 g/cm^3. Compositions and dimensions were obtained through communications with Landauer (Private communication with Professor Mark Akselrod), analysis of the micro-CT data and weight measurements of the detector disk. To identify the separate contributions from detector disk composition and dosimeter geometry to the angular dependency of the response, further simulations were performed with the composition of the detector disk set to pure Al_2O_3 and water as well as with all elements of the simulation geometry set to water.

In all simulations, a 10 × 10 cm^2 6 MV photon beam was simulated incident at the surface of the water phantom. The energy spectrum of the simulated photon beam was derived from a previous MC model of the Elekta Synergy linear accelerator used in the experimental portion of this work.[23] The class "G4PSDoseDeposit" was used to score the dose deposited in the sensitive layer. Range cuts of 1 mm and 50 μm were set for photons and electrons, respectively. The physics list "emstandard_option3" was activated. Relative responses for the dosimeter were calculated for each orientation as ratios of the collected dose at that orientation relative to the dose at normal incidence.

Simulations were performed on the Victorian Partnership for Advanced Computing (VPAC) "Trifid" cluster. The Trifid

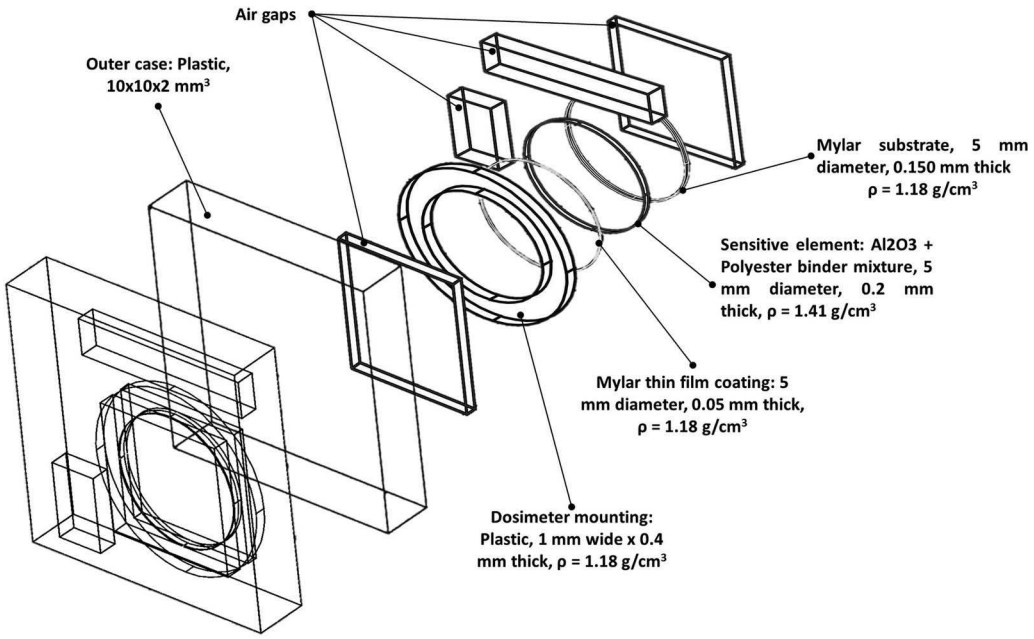

FIG. 6. Details of the geometry used for Monte Carlo simulations (export from GEANT4): wireframe (lower left) and exploded view. The exploded view shows the components of the dosimeter with dimensions, materials, and densities.

cluster is a large Intel system.[24] Trifid has 180 compute nodes, with a total of 2880 cores and HPL (High Performance Linpack) rating of 45.9 TFLOPS. For each angle and both setups (rotation perpendicular and parallel), 10^{10} initial photon histories were simulated using 200 nodes or 5×10^8 histories per simulation per angle. Simulations took approximately 40 h to complete and yielded a standard uncertainty of less than 0.5% on average.

3. RESULTS

3.A. Angular dependence of dosimeter

Figure 7 shows the results for both the measurements and the Monte Carlo simulations with the detector oriented as in Setup 1 at depth of 3 cm and normalized to the response at 180° (normal to beam direction).

In the Monte Carlo simulations for Setup 1 at 3 cm depth, the largest differences in response can be seen to occur for the 90° and 270° angles. A drop of 1.8% ± 0.3% and 2.0% ± 0.2% was found for 90° and 270°, respectively. The measurement results demonstrated a reduction in response of 1.1% ± 0.7% and 1.3% ± 0.6% at these angles. Differences between the Monte Carlo simulations and measurements were 0.7% for both, 90° and 270°.

Figure 8 shows the results for the measurements and Monte Carlo simulations for Setup 1 at a depth of 10 cm. The largest reduction in response was again found for angles 90° and 270°, with reductions of 2.2% ± 0.3% for both angles. Correspondingly, the measurement results showed a drop of 2.1% ± 0.9% and 1.1% ± 0.5% for 90° and 270°, respectively. Differences between the Monte Carlo simulation and experimental results were 0.3% and 1.1% for 90° and 270°, respectively.

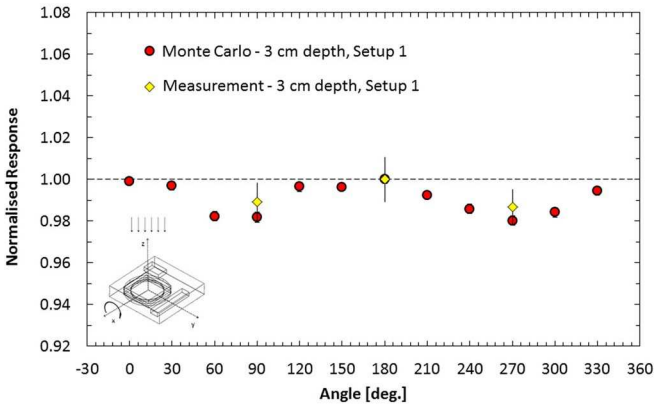

FIG. 7. Relative response of the detector for Setup 1 at 3 cm depth. Measurement results are shown as diamonds and Monte Carlo results are shown as circles. Data are normalized to 180°. Error bars show the standard uncertainty for measurement and Monte Carlo simulations, respectively. In addition to the shown statistical uncertainty, a systematic uncertainty of up to 0.7% can be estimated for the Monte Carlo simulations as discussed in Sec. 3.B. The schematic in the bottom left hand corner indicates the orientation and axis of rotation of the dosimeter with respect to the beam. Data shown in all figures are displayed with the error bars representing the statistical standard uncertainty. For all diagrams the same scale on the *y* axis was used for better comparison.

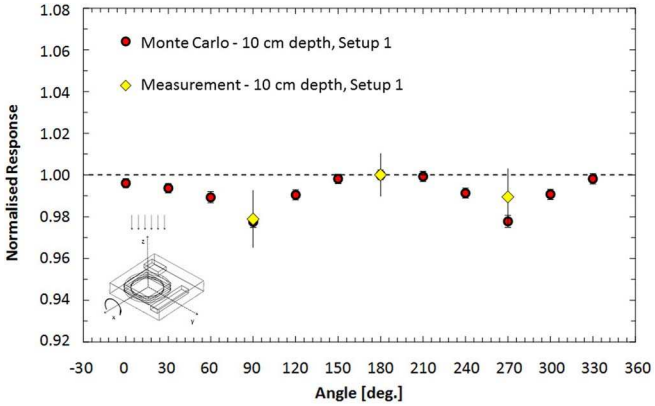

FIG. 8. Relative response of the detector for Setup 1 at 10 cm depth. Measurement results are shown as diamonds and Monte Carlo results are shown as circles. Data are normalized to 180°. Error bars show the standard uncertainty for experimental and Monte Carlo simulations, respectively. In addition to the shown statistical uncertainty, a systematic uncertainty of up to 0.7% can be estimated for the Monte Carlo simulations as discussed in Sec. 3.B. The schematic in the bottom left hand corner indicates the orientation and axis of rotation of the dosimeter with respect to the beam.

Overall, the average response for a 90° deviation from the "regular," perpendicular beam angle was found to be 1.4% ± 0.7% through measurement and 2.1% ± 0.3% through Monte Carlo simulation. The uncertainties represent one standard deviation of the measured and simulated values, respectively. Figure 9 shows the angular response of the dosimeter in Setup 2. Results from measurements and Monte Carlo simulations both show a reduced angular response compared to Setup 1. The detector response is within 1% for all angles. The largest variation found was 0.55% ± 0.4% (45°) and 0.90% ± 0.3% (90°) for the simulation and measurement results, respectively. Both these variations were at 3 cm depth. Figure 10 shows the response of the dosimeter for Setup 2 normalized to the response at optimal exposure conditions, i.e.,

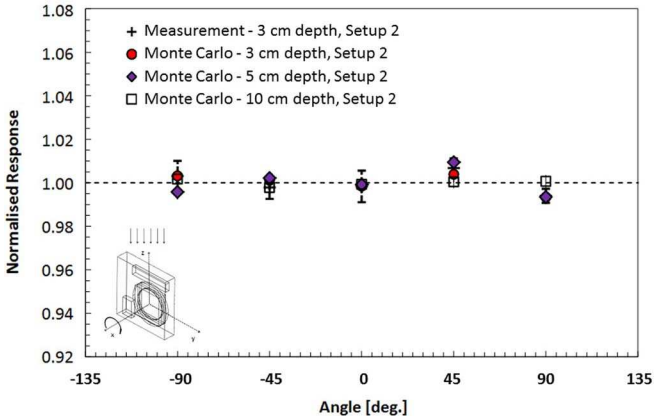

FIG. 9. Relative response of the detector for Setup 2. Measurement results at 3 cm depth are shown as crosses and Monte Carlo simulation results at 3, 5, and 10 are shown as circles, diamonds, and squares, respectively. Data are normalized to 0°. The dashed error bars correspond to the standard uncertainty of the averaged measurements. Uncapped error bars show the standard uncertainty in the Monte Carlo simulations. The schematic in the bottom left hand corner indicates the orientation and axis of rotation of the dosimeter with respect to the beam.

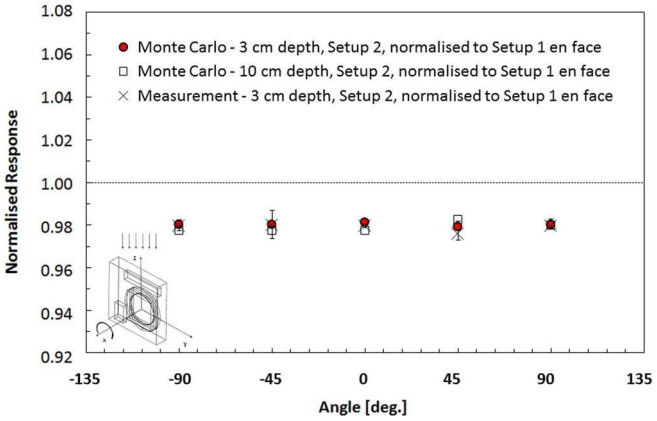

FIG. 10. Response of dosimeters aligned as in Setup 2 normalized to the response at optimal exposure conditions, i.e., plane of dosimeter enface to beam (Setup 1). Measurement results at 3 cm depth are shown as crosses and Monte Carlo simulation results at 3 and 10 are shown as circles and squares, respectively. The dashed error bars correspond to the standard uncertainty of the averaged measurements. Uncapped error bars show the standard uncertainty in the Monte Carlo simulations. The schematic in the bottom left hand corner indicates the orientation and axis of rotation of the dosimeter with respect to the beam.

plane of dosimeter enface to beam, Setup 1 (0° or 180°). Measurement results at 3 cm depth and results from simulations at 3 and 10 cm depth are displayed.

3.B. Analysis of geometrical and compositional contributions

The angular response of the dosimeter is critically sensitive to the exact composition of the detector disk. Results of the investigation of the impact of this composition are shown in Fig. 11 for Setup 1 and a 3 cm depth of the dosimeter. As a starting point, all materials have been simulated as water. In the next step, the dosimeter was simulated in realistic detail.

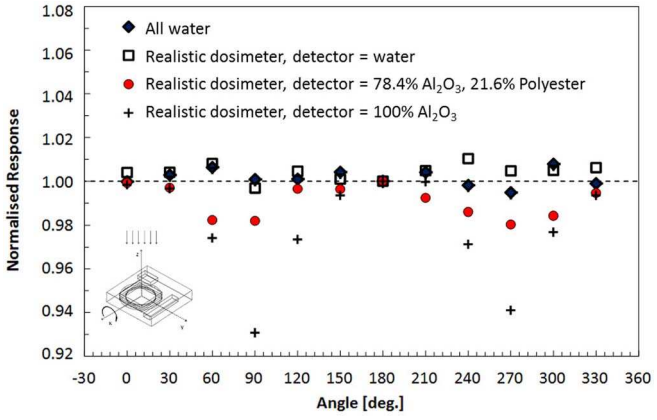

FIG. 11. Monte Carlo simulated angular response of the dosimeter for different compositions (Setup 1 at 3 cm depth). Results are shown for an all-water geometry (diamonds) and for three geometries with realistic simulation of all dosimeter details but different materials for the detector disk: water (squares), 78.4% Al_2O_3 21.6% polyester (as assumed to be the real composition, circles), 100% Al_2O_3 (crosses). Data are normalized to 180°. Error bars have been removed for improved clarity. Standard statistical uncertainty for the Monte Carlo simulations is about 0.3%–0.4%.

The material of the detector disk was simulated with different materials, while all other components were kept constant. Results are shown for water, a composite of 78.4% Al_2O_3 and 21.6% polyester (which is assumed to be the real composition, as described earlier), and 100% Al_2O_3. For clarity error bars have been omitted. All data points have a standard statistical uncertainty of 0.3%–0.4%.

Responses for the all water geometry and detector disk set to water are flat within the uncertainties of the simulation. Simulating the detector disk comprised solely of Al_2O_3 ($\rho = 3.96$ g/cm^3) the dosimeter under responds for up to 7% (90°) relative to 180°. Using the assumed real composition of the detector disk (78.4% Al_2O_3 and 21.6% polyester, $\rho = 1.41$ g/cm^3), the under response of the dosimeter is limited to 2.2%, for both 90° and 270°, as also reported in Sec. 3.A.

The strong dependence of the angular response on the detector composition adds a systematic uncertainty to the results of the Monte Carlo simulations in Sec. 3.A. Based on our investigations into detector material distribution and density we estimate the uncertainty in the composition of the detector material to be 3%. This leads to a systematic uncertainty of 0.7% in the max angular response. The uncertainty has been noted in the relevant figure captions.

4. DISCUSSION

Understanding the variation of dosimeter response with radiation incidence angle is valuable for any dosimeter. For nanoDot dosimeters this understanding is important if the dosimeter is placed in a phantom, for clinical QA or in an audit situation, to assess dose of a multibeam treatment scenario. Furthermore, for *in vivo* dosimetry during treatment, placement of the dosimeter on the skin will almost never be at complete normal incidence to the beam direction.

This study has found a 2% reduction in the response of the nanoDot dosimeter at 90° and 270° compared to 0° for 6 MV photons. The results are supported by measurements and Monte Carlo simulations at 3 and 10 cm depth. It should be noted that all angular responses determined by measurement were slightly smaller than the corresponding ones found with Monte Carlo simulation. We attribute this to the systematic uncertainty in the Monte Carlo results due to the uncertainty of the exact composition of the detector disk. The measured results are in our estimate the more reliable measure of the angular response giving an overall response of 1.4% ± 0.7% for Setup 1.

The Monte Carlo simulations for Setup 1 at 3 cm depth (Fig. 7) show some nonsymmetrical results between the 30° and 120° angles, while above 180° the response appears to be more symmetrical. The effect is small but could be real as the deviations from symmetry are larger than the statistical standard uncertainty. These deviations are possibly due to the asymmetry of the dosimeter geometry about the center of the detector disk as best appreciated in Fig. 5(d). The effect was not observed for the extreme case of the 100% Al_2O_3 detector disk (Fig. 11). It was also absent for the simulations at 10 cm depths (Fig. 8). While the latter could be due to broader

angular distribution of photons at depth, it is well possible that the nonsymmetrical results between the 30° and 120° angles for the Setup 1 simulations at 3 cm depth are caused by simulation uncertainties. Either way, the effect will have very limited if any practical impact, as the maximum deviation in response, which was found at 90°, is the important number to consider.

The angular response found in this work is smaller than the one reported by Kerns *et al.*[18] who also performed experiments and Monte Carlo simulations and found that the dosimeters under respond by up to 4% (6 MV photons at approximately 10 cm depth) for non-normal incidence of the beam (90°) compared to normal beam incidence (0°). The difference in the Monte Carlo simulation results of this work compared to Kerns *et al.* can be explained by the material composition of the sensitive layer of the detector used in the simulations. Kerns *et al.* assumed a detector consisting of 100% Al_2O_3. As discussed above the detector actually consists of 78.4% Al_2O_3 and 21.6% polyester, which was used in this model of this study. When changing the composition of the detector to 100% Al_2O_3 the response increases significantly as shown in Fig. 11. An additional consideration when comparing both Monte Carlo studies are the statistical uncertainties. Uncertainties for Kerns' Monte Carlo study were of the order of 2% (6 MV MC "with air" model).[18] The statistical uncertainty in this study is lower due to the large number of histories (10^{10}) simulated. It amounts to 0.2%–0.3% for the 6 MV "Setup 1" simulations at 3 and 10 cm depth.

The difference in the measurement results of this work compared to Kerns *et al.* can be explained by the design of the dosimeter holder. Kerns *et al.* did not actually place the center of the detector at the center of rotation for their measurements. They used an average of two dosimeters which were equal distances away from the axis of rotation of their phantom, as can be seen in Fig. 3 of their paper. The first author, James Kern, acknowledges problems with the measurement setup in his thesis and concludes that "more studies should be performed to solidify the results, with careful consideration of the setup and uncontrolled variables to isolate the angular dependence."[25] Such study has been presented here.

In a study covering several aspects of OSLD, Kim *et al.*[19] report an angular dependence of the response of the dosimeter as a drop in signal of 2.4% for 75° incident angle vs 0° (straight on) for 6 MV photon beams at 15 cm depth. The authors describe the placement of the OSLD with "at the center of the cylindrical phantom, which was a 30 cm in diameter virtual water phantom provided by TomoTherapy, Inc."[19] No details were provided on how the dosimeters were placed within this phantom. The current version of the TomoPhantom, often referred to as Cheese Phantom (Accuray Inc, Sunnyvale, CA), does not accommodate for placement of nanoDots at its center without some custom additions. Given the dependence of the measured angular response of the dosimeter on small details of the measurement setup, as described above, it is difficult to evaluate the results of Kim *et al.*[19] However, as their 75° data point (2.4% under response) has a reported uncertainty of 5.7% (one standard deviation), it can be considered to not contradict the findings of this study.

Jursinic[1] performed comprehensive measurements in water equivalent custom phantoms with the dosimeter positioned at approximately 1.8 cm depth. He concluded that nanoDot OSLDs exhibit no angular dependence within the measurement uncertainty, which he specified with 0.9%. As described in Sec. 1, the data for the angular response reported by Jursinic actually deviate from unity by up to 2% in both directions over the 24 angles investigated. No specific relationship between the response and the angle can be seen, and it is not commented on why this deviation occurs. Jursinic performed the study with a single OSLD and described in the caption of the figure "The OSLD and TLD were zeroed, irradiated, and read for each incident angle."[1] It is not reported how many repeats were done for each angle and how the provided measurement uncertainty of 0.9% was determined. Jursinic stated that he allowed 8–15 min wait after the end of an irradiation before readout. As the OSLD signal still fades at that time point,[5] small inconsistencies in timing might have contributed to the deviations. Either way, the overall uncertainty of Jursinic's angular response data can be estimated to be 2%–3%. Therefore, the angular dependence of the nanoDot OLSD as determined in this work is within the uncertainty of Jursinic's data.

A novel method for mitigating the angular response of the nanoDot dosimeter has been presented in this work. By mounting the dosimeter as in Setup 2 with the plane of the dosimeter parallel to the beam direction the angular response of the dosimeter is reduced to within the measurement uncertainty. This result has particular implications for measurements at depth for multifield radiotherapy with coplanar beams. One can negate the angular response and simply apply a single correction factor for the dosimeter which corrects for the response at 90° relative to 0°, as illustrated in Fig. 10. Alternatively one could calibrate the dosimeters in the 90° position.

5. CONCLUSION

Precisely performed measurements of the nanoDOT OSLD for 6 MV photons at 3 and 10 cm depth in a phantom showed an angular dependence of the response of the dosimeter of up to 2% relative to the response with the plane of the dosimeter normal to the beam direction. Monte Carlo simulations using realistic density and composition of the active material supported these findings and allowed for further investigation into the cause of the angular response.

This under response needs to be considered for measurements involving other than normal incident beams angles. This applies in particular to clinical *in vivo* measurements where the orientation of the dosimeter is dictated by clinical circumstances and cannot be optimized as otherwise suggested here.

Changing the orientation of the dosimeter so that a coplanar beam arrangement always hits the disk shaped detector material from the thin side (Setup 2) mitigates the angular response of the dosimeter from the beam angle by always ensuring the same path length through the sensitive layer irrespective of the angle of incidence. This reduces the angular

dependence of the response to within the measurement uncertainty of about 1%. This improvement makes the dosimeter more attractive for phantom based clinical measurements with multiple coplanar beams in phantoms, as the overall measurement uncertainty has been reduced. Similarly, phantom based postal audits with multiple coplanar beams can transition from the traditional TLD to the more accurate and convenient OSLD.

ACKNOWLEDGMENTS

The authors would like to thank Peter Jenkinson and Wayne Patullo for the construction and the engineering support in making the custom OSLD holders. The authors would also like to acknowledge Professor Mark Akselrod for providing detailed information regarding the composition of the dosimeter. The Australian Clinical Dosimetry Service is a joint initiative between the Australian Department of Health and the Australian Radiation Protection and Nuclear Safety Agency.

[a]Author to whom correspondence should be addressed. Electronic mail: Joerg.Lehmann@sydney.edu.au

[1]P. A. Jursinic, "Characterization of optically stimulated luminescent dosimeters, OSLDs, for clinical dosimetric measurements," Med. Phys. **34**, 4594–4604 (2007).
[2]C. S. Reft, "The energy dependence and dose response of a commercial optically stimulated luminescent detector for kilovoltage photon, megavoltage photon, and electron, proton, and carbon beams," Med. Phys. **36**, 1690–1699 (2009).
[3]J. Aguirre, P. Alvarez, C. Amador, A. Tailor, D. Followill, and G. Ibbott, "Validation of the commissioning of an optically stimulated luminescence (OSL) system for remote dosimetry audits," Med. Phys. **37**, 3428 (2010).
[4]P. A. Jursinic, "Changes in optically stimulated luminescent dosimeter (OSLD) dosimetric characteristics with accumulated dose," Med. Phys. **37**, 132–140 (2010).
[5]L. Dunn, J. Lye, J. Kenny, J. Lehmann, I. Williams, and T. Kron, "Commissioning of optically stimulated luminescence dosimeters for use in radiotherapy," Radiat. Meas. **51–52**, 31–39 (2013).
[6]P. A. Jursinic and C. J. Yahnke, "In vivo dosimetry with optically stimulated luminescent dosimeters, OSLDs, compared to diodes; the effects of buildup cap thickness and fabrication material," Med. Phys. **38**, 5432–5440 (2011).
[7]S. W. S. McKeever, "Optically stimulated luminescence: A brief overview," Radiat. Meas. **46**, 1336–1341 (2011).
[8]E. G. Yukihara, G. Mardirossian, M. Mirzasadeghi, S. Guduru, and S. Ahmad, "Evaluation of Al_2O_3:C optically stimulated luminescence (OSL) dosimeters for passive dosimetry of high-energy photon and electron beams in radiotherapy," Med. Phys. **35**, 260–269 (2008).
[9]B. Hu, Y. Wang, and W. Zealey, "Performance of Al2O3:C optically stimulated luminescence dosimeters for clinical radiation therapy applications," Australas Phys. Eng. Sci. Med. **32**, 226–232 (2009).
[10]J. V. Valiyaparambil and S. M. Mallya, "Characterization of an optically stimulated dosimeter for dentomaxillofacial dosimetry," Oral. Surg. Oral. Med. Oral. Pathol. Oral. Radiol. Endod. **112**, 793–797 (2011).
[11]A. Viamonte, L. A. da Rosa, L. A. Buckley, A. Cherpak, and J. E. Cygler, "Radiotherapy dosimetry using a commercial OSL system," Med. Phys. **35**, 1261–1266 (2008).
[12]I. Mrčela, T. Bokulić, J. Izewska, M. Budanec, A. Fröbe, and Z. Kusić, "Optically stimulated luminescence in vivo dosimetry for radiotherapy: Physical characterization and clinical measurements in (60)Co beams," Phys. Med. Biol. **56**, 6065–6082 (2011).
[13]E. G. Yukihara, E. M. Yoshimura, T. D. Lindstrom, S. Ahmad, K. K. Taylor, and G. Mardirossian, "High-precision dosimetry for radiotherapy using the optically stimulated luminescence technique and thin Al_2O_3:C dosimeters," Phys. Med. Biol. **50**, 5619–5628 (2005).
[14]E. G. Yukihara, P. B. R. Gasparian, G. O. Sawakuchi, C. Ruan, S. Ahmad, C. Kalavagunta, W. J. Clouse, N. Sahoo, and U. Titt, "Medical applications of optically stimulated luminescence dosimeters (OSLDs)," Radiat. Meas. **45**, 658–662 (2010).
[15]D. S. Followill, D. R. Evans, C. Cherry, A. Molineu, G. Fisher, W. F. Hanson, and G. S. Ibbott, "Design, development, and implementation of the radiological physics center's pelvis and thorax anthropomorphic quality assurance phantoms," Med. Phys. **34**, 2070–2076 (2007).
[16]J. Lye, L. Dunn, J. Kenny, J. Lehmann, T. Kron, C. Oliver, D. Butler, A. Alves, P. Johnston, R. Franich, and I. Williams, "Remote auditing of radiotherapy facilities using optically stimulated luminescence dosimeters," Med. Phys. **41**(3), 032102 (10pp.) (2014).
[17]Landauer InLight nanoDOT (available URL: http://www.landauer.com/uploadedFiles/InLight_nanoDot_FN.pdf).
[18]J. R. Kerns, S. F. Kry, N. Sahoo, D. S. Followill, and G. S. Ibbott, "Angular dependence of the nanoDot OSL dosimeter," Med. Phys. **38**, 3955–3962 (2011).
[19]D. W. Kim, W. K. Chung, D. O. Shin, M. Yoon, U. J. Hwang, J. E. Rah, H. Jeong, S. Y. Lee, D. Shin, S. B. Lee, and S. Y. Park, "Dose response of commercially available optically stimulated luminescent detector, Al_2O_3:C for megavoltage photons and electrons," Radiat. Prot. Dosim. **149**, 101–108 (2012).
[20]S. Agostinelli *et al.*, "Geant4—A simulation toolkit," Nucl. Instrum. Methods Phys. Res. A **506**, 250–303 (2003).
[21]P. Charles, S. Crowe, T. Kairn, J. Kenny, J. Lehmann, J. Lye, L. Dunn, B. Hill, R. Knight, and C. Langton, "The effect of very small air gaps on small field dosimetry," Phys. Med. Biol. **57**, 6947 (2012).
[22]M. S. Akselrod, V. S. Kortov, and E. A. Gorelova, "Preparation and properties of alpha-Al_2O_3:C," Radiat. Protect. Dosim. **47**, 159–164 (1993).
[23]J. E. Lye, D. J. Butler, G. Ramanathan, and R. D. Franich, "Spectral differences in 6 MV beams with matched PDDs and the effect on chamber response," Phys. Med. Biol. **57**, 7599–7614 (2012).
[24]Trifid Cluster (available URL: http://www.vpac.org/news/2013/new-cluster-trifid).
[25]J. R. Kerns "Characterization of optically stimulated luminescent detectors in photon and proton beams for use in anthropomorphic phantoms," University of Texas Graduate School of Biomedical Sciences (2010) (available URL: http://digitalcommons.library.tmc.edu/utgsbs_dissertations/66/).